Nonlinear Processes
in Geophysics

An analytical model of the evolution of a Stokes wave and its two Benjamin–Feir sidebands on nonuniform unidirectional current

I. V. Shugan[1,2]**, H. H. Hwung**[1]**, and R. Y. Yang**[1]

[1]International Wave Dynamics Research Center, National Cheng Kung University, Tainan City, Taiwan
[2]Prokhorov General Physics Institute, Russian Academy of Sciences, Moscow, Russia

Correspondence to: I. V. Shugan (ishugan@rambler.ru)

Abstract. An analytical weakly nonlinear model of the Benjamin–Feir instability of a Stokes wave on nonuniform unidirectional current is presented. The model describes evolution of a Stokes wave and its two main sidebands propagating on a slowly varying steady current. In contrast to the models based on versions of the cubic Schrödinger equation, the current variations could be strong, which allows us to examine the blockage and consider substantial variations of the wave numbers and frequencies of interacting waves. The spatial scale of the current variation is assumed to have the same order as the spatial scale of the Benjamin–Feir (BF) instability. The model includes wave action conservation law and nonlinear dispersion relation for each of the wave's triad. The effect of nonuniform current, apart from linear transformation, is in the detuning of the resonant interactions, which strongly affects the nonlinear evolution of the system.

The modulation instability of Stokes waves in nonuniform moving media has special properties. Interaction with countercurrent accelerates the growth of sideband modes on a short spatial scale. An increase in initial wave steepness intensifies the wave energy exchange accompanied by wave breaking dissipation, resulting in asymmetry of sideband modes and a frequency downshift with an energy transfer jump to the lower sideband mode, and depresses the higher sideband and carrier wave. Nonlinear waves may even overpass the blocking barrier produced by strong adverse current. The frequency downshift of the energy peak is permanent and the system does not revert to its initial state. We find reasonable correspondence between the results of model simulations and available experimental results for wave interaction with blocking opposing current. Large transient or freak waves with amplitude and steepness several times those of

normal waves may form during temporal nonlinear focusing of the waves accompanied by energy income from sufficiently strong opposing current. We employ the model for the estimation of the maximum amplification of wave amplitudes as a function of opposing current value and compare the result obtained with recently published experimental results and modeling results obtained with the nonlinear Schrödinger equation.

1 Introduction

The problem of the interaction of a nonlinear wave with slowly varying current remains an enormous challenge in physical oceanography. In spite of numerous papers devoted to the analysis of the phenomenon, some of the relatively strong effects still await a clear description. The phenomenon can be considered the discrete evolution of the spectrum of the surface wave under the influence of nonuniform adverse current. Experiments conducted by Chavla and Kirby (1998, 2002) and Ma et al. (2010) revealed that sufficiently steep surface waves overpass the barrier of strong opposing current on the lower resonant Benjamin–Feir sideband. These reports highlight that the frequency step of a discrete downshift coincides with the frequency step of modulation instability; i.e., after some distance of wave run, the maximum of the wave spectrum shifts in frequency to the lower sideband. The intensive exchange of wave energy produces a peak spectrum transfer jump, which is accompanied by essential wave breaking dissipation. The spectral characteristics of the initially narrowband nonlinear surface wave packet

dramatically change and the spectral width is increased by dispersion induced by the strong nonuniform current.

This paper presents a weakly nonlinear model of the Benjamin–Feir (BF) instability on nonuniform slowly varying current.

The stationary nonlinear Stokes wave is unstable in response to perturbation of two small neighboring sidebands. The initial exponential growth of the two dominant sidebands at the expense of the primary wave gives rise to an intriguing Fermi–Pasta–Ulam recurring phenomenon of the initial state of wave trains. This phenomenon is characterized by a series of modulation–demodulation cycles in which initially uniform wave trains become modulated and then demodulated until they are again uniform (Lake and Yuen, 1978). However, when the initial slope is sufficiently steep, the longtime evolution of the wave train is different. The evolving wave trains experience strong modulations followed by demodulation, but the dominant component is the component at the frequency of the lower sideband of the original carrier. This is the temporary frequency downshift phenomenon. In systematic well-controlled experiments, Tulin and Waseda (1999) analyzed the effect of wave breaking on downshifting, high-frequency discretized energy, and the generation of continuous spectra. Experimental data clearly show that the active breaking process increases the permanent frequency downshift in the latter stages of wave propagation.

The BF instability of Stokes waves and its physical applications have been studied in depth over the last few decades; a long but incomplete list of research is Lo and Mei (1985), Duin (1999), Landrini et al., 1998; Osborne et al. (2000), Trulsen et al. (2000), Janssen (2003), Segur et al. (2005), Shemer et al. (2002), Zakharov et al. (2006), Bridges and Dias (2007), Hwung, Chiang and Hsiao (2007), Chiang and Hwung (2010), Shemer (2010), and Hwung et al. (2011). The latter stages of one cycle of the modulation process have been much less investigated, and many physical phenomena that have been observed experimentally still require extended theoretical analysis.

Modulation instability and the nonlinear interactions of waves are strongly affected by variable horizontal currents. Here, we face another fundamental problem of the mechanics of water waves–interactions with slowly varying current. The effect of opposing current on waves is a problem of practical importance at tidal inlets and river mouths.

Even linear refraction of waves on currents can affect the wave field structure in terms of the direction and magnitude of waves. Waves propagating against an opposing current may have reduced wavelength and increased wave height and steepness.

If the opposing current is sufficiently strong, then the absolute group wave velocity in the stationary frame will become zero, resulting in the waves being blocked. This is the most intriguing phenomenon in the problem of wave–current interaction (Phillips, 1977). The kinematic condition for wave blocking can be written as

$$C_g + U(X) \rightarrow 0,$$

where C_g is the intrinsic group velocity of waves in a moving frame and $U(X)$ is slowly varying horizontal current, with X being the horizontal coordinate in the direction of wave propagation. Waves propagating against opposing current are stopped if the magnitude of the current, in the direction of wave propagation, exceeds the group velocity of the oncoming waves. This characteristic feature of wave blocking has drawn the interest of oceanographers and coastal engineers alike for its ability to be used as signature patterns of underlying large-scale motion (e.g., fresh water plumes and internal waves) and for the navigational hazard it poses. Smith (1975), Peregrine (1976), and Lavrenov (1998) analyzed refraction/reflection around a blocking region and obtained a uniformly valid linearized solution, including a short reflecting wave.

The linear modulation model has a few serious limitations. The most important is that the model predicts the blocking point according to the linear dispersion relation and cannot account for nonlinear dispersive effects. Amplitude dispersion effects can considerably alter the location of wave blocking predicted by linear theory, and nonlinear processes can adversely affect the dynamics of the wave field beyond the blocking point.

Donato et al. (1999), Stocker and Peregrine (1999), and Moreira and Peregrine (2012) conducted fully nonlinear computations to analyze the behavior of a train of water waves in deep water when meeting nonuniform currents, especially in the region where linear solutions become singular. The authors employed spatially periodic domains in numerical study and showed that adverse currents induce wave steepening and breaking. A strong increase in wave steepness is observed within the blocking region, leading to wave breaking, while wave amplitudes decrease beyond this region. The nonlinear wave properties reveal that at least some of the wave energy that builds up within the blocking region can be released in the form of partial reflection (which applies to very gentle waves) and wave breaking (even for small-amplitude waves).

The enhanced nonlinear nature of sideband instabilities in the presence of strong opposing current has also been confirmed by experimental observations. Chavla and Kirbi (2002) experimentally showed that the blockage phenomenon strongly depends on the initial wave steepness; i.e., waves are blocked when the initial slope is small ($ak < 0.16$, where a and k are the wave amplitude and wave number, respectively). When the slope is sufficiently steep ($ak > 0.22$), the behavior of waves is principally different; i.e., waves are blocked only partly and frequency-downshifted waves overpass the blocking barrier. The lower sideband mode may dramatically increase; i.e., the amplitude rises several times within a distance of a few wavelengths.

Wave propagation against nonuniform opposing currents was recently investigated in experiments conducted by Ma et al. (2010). Results confirm that opposing current not only increases the wave steepness but also shortens the wave energy transfer time and accelerates the development of sideband instability. A frequency downshift, even for very small initial steepness, was identified. Because of the frequency downshift, waves are more stable and have the potential to grow higher and propagate more quickly. The ultimate frequency downshift increases with an increase in initial steepness.

The wave modulation instability with coexisting variable current is commonly described theoretically by employing different forms of the modified nonlinear Schrödinger (NLS) equation. Gerber (1987) used the variational principle to derive a cubic Schrödinger equation for a nonuniform medium, limiting to potential theory in one horizontal dimension. Stocker and Peregrine (1999) extended the modified nonlinear NLS equation of Dysthe (1979) to include a prescribed potential current. Hjelmervik and Trulsen (2009) derived an NLS equation that includes waves and currents in two horizontal dimensions allowing weak horizontal shear. The horizontal current velocities are assumed just small enough to avoid collinear blocking and reflection of the waves.

Even though the frequency downshift and other nonlinear phenomena were observed in previous experimental studies on wave–current interactions, the theoretical description of the modulation instability of waves on opposing currents is not yet complete. An interaction of an initially relatively steep wave train with strong current nevertheless may abruptly transfer energy between the resonantly interacting harmonics. Such wave phenomena are beyond the applicability of NLS-type models and await a theoretical description.

Another topic of practical interest in wave–current interaction problems is the appearance of large transient or freak waves with great amplitude and steepness owing to the focusing mechanism (e.g., Peregrine, 1976; Lavrenov, 1998; White and Fornberg, 1998; Kharif and Pelinovsky, 2006; Janssen and Herbers, 2009; Ruban, 2012; Osborne, 2001). Both nonlinear instability and refractive focusing have been identified as mechanisms for extreme-wave generation and these processes are generally concomitant in oceans and potentially act together to create giant waves.

Toffoli et al. (2013) showed experimentally that an initially stable surface wave can become modulationally unstable and even produce freak or giant waves when meeting negative horizontal current. Onorato et al. (2011) suggested an equation for predicting the maximum amplitude A_{max} during the wave evolution of currents in deep water. Their numerical results revealed that the maximum amplitude of the freak wave depends on U/C_g, where U is the velocity of the current and C_g is the group velocity of the wave packet.

Recently, Ma et al. (2013) experimentally investigated the maximum amplification of the amplitude of a wave on opposing current having variable strength at an intermediate water depth. They mentioned that theoretical values of amplifica-

tion (Onorato et al., 2011; Toffoli et al., 2013) are essentially overestimated, probably owing to the effects of finite depth and wave breaking.

To address the above-mentioned problems, we present the model of BF instability in the presence of horizontal slowly varying current of variable strength. We analyze the interactions of a nonlinear surface wave with sufficiently strong opposing blocking current and the frequency downshifting phenomenon. The maximum amplification of the amplitude of surface waves is estimated in dependence on relative strength of opposing current. We take into account the dissipation effects due to wave breaking by utilizing the Tulin wave breaking model (Tulin, 1996; Hwung et al., 2011). The results of model simulations are compared with available experimental results and theoretical estimations.

We employ simplified 3-wave model in the presence of significant opposite current. In the meanwhile, the evolution of the wave spectrum in the absence of breaking includes energy exchange between the carrier wave and two main resonant sidebands and spreading of the energy to higher frequencies. Inclusion of higher frequency free waves in the Zakharov, modified Schrödinger or Dysthe equations is crucial, since the asymmetry of the lower and the upper sideband amplitudes at peak modulation in non-breaking case results from that. The temporal spectral downshift has been predicted by computations made by the Dysthe equations (Lo and Mei, 1985; Trulsen and Dysthe, 1990; Hara and Mei, 1991; Dias and Kharif, 1999) for a much higher number of excited waves, the same prediction was also made by simulations of fully nonlinear equations (Tanaka, 1990; Slunyaev and Shrira, 2013). Such a conclusion can be made regarding to developing of modulation instability in calm water.

Nevertheless, the experimental results of Chavla and Kirby (2002) and Ma et al. (2010) on the modulation instability under the influence of adverse current show that energy spectrum is mostly concentrated in the main triad of waves and high-frequency discretized energy spreading is depressed due to the short-wave blocking by the strong enough adverse current. Higher side band modes have also prevailed energy loss during wave breaking (Tulin and Waseda, 1999). That is why we hope that our simplified model still has potentiality to adequately describe some prominent features of wave dynamics on the adverse current.

The paper consists of five sections. General modulation equations are derived in Sect. 2. Section 3 is devoted to stationary nondissipative solutions for adverse and following nonuniform currents and various initial steepness of the surface wave train. We calculate the maximum amplitude amplification in dependence from relative strength of opposing current and compared it with available experimental and theoretical results (Toffoli et al., 2013; Ma et al., 2013). The interaction of steep surface waves with strong adverse current under wave-blocking conditions including wave breaking effects is presented in Sect. 4. Modeling results are compared with the results of a series of experiments conducted

by Chavla and Kirby (2002) and Ma et al. (2010). Section 5 summarizes our final conclusions and discussion.

2 Modulation equations for one-dimensional interaction

The first set of complete equations that describe short waves propagating over nonuniform currents of much larger scale were given by Longuet-Higgins and Stewart (1964). Wave energy is not conserved, and the concept of "radiation stress" was introduced to describe the average momentum flux in terms that govern the interchange of momentum with the current. In this model, it is also justifiable to neglect the effect of momentum transfer on the form of the surface current because it is an effect of the highest order (Stocker and Peregrine, 1999).

We construct a model of the current effect on the modulation instability of a nonlinear Stokes wave by making the following assumptions:

i. Surface waves and current propagate along a common x-direction.

ii. By a_c, k_c, and ω_c we denote the characteristic amplitude, wave number, and angular frequency of the surface waves. We use a small conventional average wave steepness parameter; $\varepsilon = a_c k_c \ll 1$.

iii. The characteristic spatial scale used in developing the BF instability of the Stokes wave is l_c / ε^2, where $l_c = 2\pi / k_c$ is the typical wavelength of surface waves (Benjamin and Feir, 1967). We consider slowly varying current $U(x)$ with horizontal length scale L of the same order: $L = O(l_c / \varepsilon^2)$.

iv. It is assumed that the $U(x)$ dependence is due to the inhomogeneity of the bottom profile $h(x)$, which is sufficiently deep so that the deep-water regime for surface waves is ensured; i.e., $\exp(-2k_c h) \ll 1$. The characteristic current length L at which the function $U(x)$ varies noticeably is assumed to be much larger than the depth of the fluid, $h(x) \ll L$. Under these conditions, shallow water model for the current description may be adopted: $U(x)h(x)$ is assumed to be approximately constant, and the vertical component of the steady velocity field on the surface $z = \eta(x)$ can be neglected. Correspondingly, it follows from the Bernoulli time-independent equation that the surface displacement induced by the current is small (Ruban, 2012). Such a situation can occur, for example, near river mouths or in tidal/ebb currents.

In all following equations, variables and sizes are scaled according to the above assumptions, and made dimensionless using the characteristic length and timescales of the wave field.

The dimensionless set of equations for potential motion of an ideal incompressible deep-depth fluid with a free surface in the presence of current $U(x)$ is given by the Laplace equation

$$\varphi_{xx} + \varphi_{zz} = 0, \, -h(x) < z < \varepsilon\eta(x,t). \tag{1}$$

The boundary conditions at the free surface are

$$-\eta = \varphi_t + U\varphi_x + \varepsilon \frac{1}{2}(\varphi_x^2 + \varphi_z^2), z = \varepsilon\eta(x,t), \tag{2}$$

$$\eta_t + U\eta_x + \epsilon\varphi_x\eta_x = \varphi_z, z = \epsilon\eta(x,t), \tag{3}$$

and those at the bottom are

$$\varphi \to 0, z = -h(x). \tag{4}$$

Here, $\varphi(x,z,t)$ is the velocity potential, $\eta(x,t)$ is the free-surface displacement, z is the vertical coordinate directed upward and t is time.

The variables are normalized as

$$\varphi = a_c \sqrt{\frac{g}{k_c}} \varphi' = \varepsilon \sqrt{\frac{g}{k_c^3}} \varphi', \eta = a_c \eta' = \frac{\varepsilon}{k_c} \eta',$$
$$t = \frac{1}{\sqrt{gk_c}} t', z = \frac{z'}{k_c}, x = \frac{x'}{k_c}, \tag{5}$$
$$U(Kx) = U'(K/k_c x') c_p = U'(\varepsilon^2 x') c_p,$$

where g is acceleration due to gravity, $K = 2\pi/L$, and c_p is the phase speed of the carrier wave, but the primes are omitted in Eqs. (1)–(4). Note that normalization (5) explicitly specifies the principal scales of sought functions φ and η.

The weakly nonlinear surface wave train is described by a solution to Eqs. (1)–(4), expanded into a Stokes series in terms of ε.

We will analyze the surface wave train of a particular form, which describes the development of modulation instability in the presence of current.

For calm water, the initially constant nonlinear Stokes wave with amplitude, wave number and frequency (a_1, k_1, σ_1) is unstable in response to a perturbation in the form of a pair of small waves with similar frequencies and wavenumbers: a superharmonic wave ($a_2, k_2 = k_1 + \Delta k, \sigma_2 = \sigma_1 + \Delta\sigma$) and subharmonic wave ($a_0, k_0 = k_1 - \Delta k, \sigma_0 = \sigma_1 - \Delta\sigma$). For most unstable modes, $\Delta\sigma/\sigma_1 = \varepsilon$ and $\Delta k/k_1 = 2\varepsilon$, where $\varepsilon = a_1 k_1$ is the initial steepness of the Stokes wave (Benjamin and Feir, 1967). This is the BF or modulation instability of the Stokes wave. Kinematic resonance conditions for waves in the presence of slowly varying current are the same, with one important particularity that intrinsic wave numbers and frequencies of waves in the moving frame are variable and modulated by the current.

We analyze the problem assuming the wave motion phase $\theta_i = \theta_i(x,t)$ exists for each wave in the presence of a slowly

varying current $U(x)$, and we define the local wave number k_i and absolute observed frequency ω_i as

$$k_i = (\theta_i)_x, \omega_i = \sigma_i + k_i U = -(\theta_i)_t, \quad i = 0, 1, 2. \tag{6}$$

For stationary modulation, the intrinsic frequency σ_i and wave number k_i for each wave slowly change in the presence of variable current, but the resonance condition

$$2\omega_1 \approx \omega_0 + \omega_2 \tag{7}$$

remains valid throughout the region of wave propagation owing to the stationary value of the absolute frequency for each harmonic.

The main kinematic wave parameters (σ_i, k_i) together with the first-order velocity potential amplitudes, φ_i, are considered further as slowly varying functions with typical scale, $O(\varepsilon^{-1})$, longer than the primary wavelength and period (Whitham, 1974):

$$\varphi_i = \varphi_i(\varepsilon x, \varepsilon t), k_i = k_i(\varepsilon x, \varepsilon t), \sigma_i = \sigma_i(\varepsilon x, \varepsilon t). \tag{8}$$

On this basis, we attempt to recover the effects of slowly varying current and nonlinear wave dispersion (having the same order) additional to the Stokes term with the order of wave steepness squared.

The solution to the problem, uniformly valid for $O(\varepsilon^3)$, is found by a two-scale expansion with the differentiation:

$$\frac{\partial}{\partial t} = -\sum (\sigma_i + k_i U)\frac{\partial}{\partial \theta_i} + \varepsilon \frac{\partial}{\partial T},$$
$$\frac{\partial}{\partial x} = \sum k_i \frac{\partial}{\partial \theta_i} + \varepsilon \frac{\partial}{\partial X}, T = \varepsilon t, X = \varepsilon x. \tag{9}$$

Substitution of the wave velocity potential in its linear form,

$$\varphi = \sum_{i=0}^{i=2} \varphi_i e^{k_i z} \sin \theta_i, \tag{10}$$

satisfies the Laplace Eq. (1) to the first order of ε owing to Eq. (8) and gives the additional terms of the second order $O(\varepsilon^2)$:

$$\varepsilon(2k_i\varphi_{iX} + k_{iX}\varphi_i + 2k_i k_{iX}\varphi_i z)e^{k_i z}\cos\theta_i + \ldots = 0.$$

To satisfy the Laplace equation to second order, Yuen and Lake (1982), Shugan and Voliak (1998), and Hwung et al. (2009) suggested an additional phase-shifted term with a linear and quadratic z correction in the representation of the potential function φ:

$$\varphi = \sum_{i=0}^{i=2} \left(\varphi_i e^{k_i z}\sin\theta_i - \varepsilon\left(\varphi_{iX} z + \frac{k_{iX}\varphi_i}{2}z^2\right) \right.$$
$$\left. e^{k_i z}\cos\theta_i \right) + \ldots. \tag{11}$$

Exponential decaying of the wave's amplitude with increasing $-z$ is accompanied by a second-order subsurface jet owing to slow horizontal variations in the wave number and amplitude of the wave packet.

The free-surface displacement $\eta = \eta(x, t)$ is also sought as an asymptotic series:

$$\eta = \eta_0 + \varepsilon\eta_1 + \varepsilon^2\eta_2 + \ldots, \tag{12}$$

where η_0, η_1, and η_2 are $O(1)$ functions to be determined. Using Eqs. (10) and (11) subject to the dynamic boundary condition (Eq. 2), we find the components of the free-surface displacement:

$$\eta_0 = \sum_{i=0}^{i=2} \sigma_i \varphi_i \cos\theta_i, \tag{13}$$

$$\eta_1 = -\sum_{i=0}^{i=2}(\varphi_{iT}\sin\theta_i + U\varphi_{iX}\sin\theta_i)$$
$$+ \sum_{i=0}^{i=2}\varphi_i^2 k_i^2 \cos[2\theta_i]/2 \tag{14}$$
$$+ \sum_{i=0}^{i=2}\sum_{j\neq i}^{j=2}(\sigma_i - \sigma_j)^2\sigma_i\sigma_j\varphi_i\varphi_j\cos[\theta_i - \theta_j]/2$$
$$+ \sum_{i=0}^{i=2}\sum_{j\neq i}^{j=2}(\sigma_i + \sigma_j)^2\sigma_i\sigma_j\varphi_i\varphi_j\cos[\theta_i + \theta_j]/2,$$

$$-8\eta_2 = \begin{pmatrix} \sum_{i=0}^{2}\varphi_i\sigma_i^2(3\varphi_i^2\sigma_i^5 + \sum_{j\neq i}(2\sigma_j^2 + \sigma_i^2) \\ (2\sigma_j - \sigma_i))\cos[\theta_i] - \\ \varphi_0\varphi_1^2\sigma_0\sigma_1^2(\sigma_0^2 + 2\sigma_1^2)(\sigma_0^2 - 4\sigma_0\sigma_1 + 2\sigma_1^2) \\ \cos[\theta_2 + \phi] - \\ \varphi_1^2\varphi_2\sigma_1^2\sigma_2(\sigma_2^2 + 2\sigma_1^2)(\sigma_2^2 - 4\sigma_2\sigma_1 + 2\sigma_1^2) \\ \cos[\theta_0 + \phi] - \\ 2\varphi_0\varphi_1\varphi_2\sigma_0\sigma_1\sigma_2(\sigma_0^2 + \sigma_1^2 + \sigma_2^2) \\ (\sigma_0^2 - 2\sigma_0\sigma_1 + \sigma_1^2 - 2\sigma_1\sigma_2 + \sigma_2^2)\cos[\theta_1 - \phi] \end{pmatrix}, \tag{15}$$

where ϕ is a slowly varying phase-shift difference: $\phi = 2\theta_1 - \theta_0 - \theta_2$.

Only the resonance terms for all three wave modes are included in the third-order displacement (Eq. 15).

Substitution of the velocity potential (Eq. 11) and displacement (Eqs. 13–15) into the kinematics boundary condition (Eq. 3) gives, after much routine algebra, relationships between the modulation characteristics of the resonant wave:

$$\begin{cases} \sigma_0^2 = k_0 + \varepsilon^2\sigma_0^3(\varphi_0^2\sigma_0^5 + \varphi_1^2\sigma_1^3(2\sigma_1^2 - \sigma_0\sigma_1 + \sigma_0^2) \\ +\varphi_2^2\sigma_2^3(2\sigma_2^2 - \sigma_0\sigma_2 + \sigma_0^2)) + \\ \frac{\varepsilon^2\varphi_1^2\varphi_2\sigma_1^3\sigma_2^2}{\varphi_0}(2\sigma_1^3 - 2\sigma_1^2\sigma_2 + 2\sigma_1\sigma_2^2 - \sigma_2^3)\cos[\phi]; \\ \sigma_2^2 = k_2 + \varepsilon^2\sigma_2^3(\varphi_2^2\sigma_2^5 + \varphi_0^2\sigma_0^3(2\sigma_0^2 - \sigma_0\sigma_2 + \sigma_2^2) \\ +\varphi_1^2\sigma_1^3(2\sigma_1^2 - \sigma_1\sigma_2 + \sigma_2^2)) + \\ \frac{\varepsilon^2\varphi_1^2\varphi_0\sigma_1^3\sigma_0^2}{\varphi_2}(2\sigma_1^3 - 2\sigma_0\sigma_1^2 + 2\sigma_0^2\sigma_1 - \sigma_0^3)\cos[\phi]; \\ \sigma_1^2 = k_1 + \varepsilon^2\sigma_1^3(\varphi_1^2\sigma_1^5 + \varphi_0^2\sigma_0^3(2\sigma_0^2 - \sigma_0\sigma_1 + \sigma_1^2) \\ +\varphi_2^2\sigma_2^3(\sigma_1^2 - \sigma_1\sigma_2 + 2\sigma_2^2)) + \\ \varepsilon^2\varphi_0\varphi_2\sigma_0\sigma_1^2\sigma_2(\sigma_0^4 - \sigma_0^3\sigma_1 - \sigma_0\sigma_1(\sigma_1 - \sigma_2)^2 + \\ \sigma_0^2(\sigma_1^2 - \sigma_1\sigma_2 + 2\sigma_2^2) + \sigma_2(-\sigma_1^3 + \sigma_1^2\sigma_2 - \sigma_1\sigma_2^2 + \sigma_2^3)) \\ \cos[\phi], \end{cases} \tag{16}$$

$$
\begin{cases}
[\varphi_0^2\sigma_0]_T + [(U(X) + \dfrac{1}{2\sigma_0})\varphi_0^2\sigma_0]_X = \varepsilon\varphi_1^2\varphi_2\varphi_0 \\
\quad \sigma_1^3\sigma_2^2(2\sigma_1^3 - 2\sigma_1^2\sigma_2 + 2\sigma_1\sigma_2^2 - \sigma_2^3)\sin[\phi]; \\
[\varphi_2^2\sigma_2]_T + [(U(X) + \dfrac{1}{2\sigma_2})\varphi_2^2\sigma_2]_X = \varepsilon\varphi_1^2\varphi_2\varphi_0 \\
\quad \sigma_0^2\sigma_1^3(2\sigma_1^3 - 2\sigma_0\sigma_1^2 + 2\sigma_0^2\sigma_1 - \sigma_0^3)\sin[\phi]; \\
[\varphi_1^2\sigma_1]_T + [(U(X) + \dfrac{1}{2\sigma_1})\varphi_1^2\sigma_1]_X = -\varepsilon\varphi_1^2\varphi_2\varphi_0 \\
\quad \sigma_0\sigma_1^2\sigma_2(\sigma_0^4 - \sigma_0^3\sigma_1 - \sigma_0\sigma_1(\sigma_1 - \sigma_2)^2 + \\
\quad +\sigma_0^2(\sigma_1^2 - \sigma_1\sigma_2 + 2\sigma_2^2) - \sigma_2(\sigma_1^3 - \sigma_1^2\sigma_2 \\
\quad\quad +\sigma_1\sigma_2^2 - \sigma_2^3))\sin[\phi].
\end{cases} \tag{17}
$$

The formulas (16) represent the "intrinsic" dispersion relations of the nonlinear wave for each of the harmonics in the presence of current, $U(X)$. Equation (17) yields the known wave action law with the energy exchange terms on the right side of the equations.

The obtained system of Eqs. (16) and (17) in the absence of current is similar to classical Zakharov equations for discrete wave interactions (Stiassnie and Shemer, 2005; Mei et al., 2009); it has a strong symmetry with respect to indexes zero and two. The main property of the derived modulation equations is the variability of interaction coefficients in the presence of nonuniform current.

Modulation Eqs. (16) and (17) are closed by the equations of wave phase conservation that follow from Eq. (6) as the compatibility condition (Phillips, 1977):

$$
\begin{aligned}
&k_{iT} + (\sigma_i + k_i U)_X = 0, \\
&i = 0, 1, 2.
\end{aligned} \tag{18}
$$

The derived set of nine modulation Eqs. (16)–(18) form the complete system for nine unknown functions (k_i, σ_i, φ_i, $i = 0, 1, 2$).

3　Nondissipative stationary wave modulations

Let us analyze the stationary wave solutions of the problem in Eqs. (16)–(18) supposing that all unknown functions depend on the single coordinate X. Then, after integrating Eq. (18), we have the conservation law for the absolute frequency of each wave:

$$
\begin{aligned}
&\sigma_i + k_i U = \omega_i = \text{const}, \\
&i = 0, 1, 2.
\end{aligned} \tag{19}
$$

The wave action laws for resonant components take the form

$$
\begin{cases}
[(U + \dfrac{1}{2\sigma_0})\phi_0^2\sigma_0]_X = \varepsilon\phi_1^2\phi_2\phi_0\sigma_1^3\sigma_2^2 \\
\quad (2\sigma_1^3 - 2\sigma_1^2\sigma_2 + 2\sigma_1\sigma_2^2 - \sigma_2^3)\text{Sin}[\varphi] \\
[(U + \dfrac{1}{2\sigma_2})\phi_2^2\sigma_2]_X = \varepsilon\phi_1^2\phi_2\phi_0\sigma_1^3\sigma_0^2 \\
\quad (2\sigma_1^3 - 2\sigma_0\sigma_1^2 + 2\sigma_0^2\sigma_1 - \sigma_0^3)\text{Sin}[\varphi] \\
[(U + \dfrac{1}{2\sigma_1})\phi_1^2\sigma_1]_X = -\varepsilon\phi_1^2\phi_2\phi_0\sigma_0\sigma_1^2\sigma_2 \\
\quad (\sigma_0^4 - \sigma_0^3\sigma_1 - \sigma_0\sigma_1(\sigma_1 - \sigma_2)^2 + \\
\quad \sigma_0^2(\sigma_1^2 - \sigma_1\sigma_2 + 2\sigma_2^2) - \sigma_2(\sigma_1^3 - \sigma_1^2\sigma_2 \\
\quad\quad +\sigma_1\sigma_2^2 - \sigma_2^3))\text{Sin}[\varphi].
\end{cases} \tag{20}
$$

To perform the qualitative analysis of the stationary problem, we suggest the law of wave action conservation flux in a slowly moving media as analogue of the three Manley–Rowe dependent integrals:

$$
\begin{cases}
\left(U + \dfrac{1}{2\sigma_2}\right)\phi_2^2\sigma_2 + \left(U + \dfrac{1}{2\sigma_0}\right)\phi_0^2\sigma_0 \\
\quad + \left(U + \dfrac{1}{2\sigma_1}\right)\phi_1^2\sigma_1 = \text{const}; \\
\frac{1}{2}\left(U + \dfrac{1}{2\sigma_1}\right)\phi_1^2\sigma_1 + \left(U + \dfrac{1}{2\sigma_0}\right)\phi_0^2\sigma_0 = \text{const}; \\
\frac{1}{2}\left(U + \dfrac{1}{2\sigma_1}\right)\phi_1^2\sigma_1 + \left(U + \dfrac{1}{2\sigma_2}\right)\phi_2^2\sigma_2 = \text{const}; \\
\left(U + \dfrac{1}{2\sigma_0}\right)\phi_0^2\sigma_0 - \left(U + \dfrac{1}{2\sigma_2}\right)\phi_2^2\sigma_2 = \text{const}.
\end{cases}
$$

These integrals follow from the system (Eq. 20) with acceptable accuracy $O(\varepsilon^4)$ for the stationary regime of modulation. The second and third relations here clearly show that the wave action flux of the side bands can grow up at the expense of the main carrier wave flux. The last relationship manifests the almost identical behavior of the main sidebands for the problem of their generation due to the Benjamin–Feir instability.

Typical behavior of wave instability in the absence of current is presented in Fig. 1a for a Stokes wave having initial steepness $\varepsilon = 0.1$. Two initially negligible side bands (II) and (III) exponentially grow at the expense of the main Stokes wave (I), and after saturation, the wave system reverts to its initial state, which is the Fermi–Pasta–Ulam recurrence phenomenon. One can see here also the characteristic spatial scale for the developing of modulation instability $O(1/(k_c\varepsilon^2))$.

The development of modulation instability on negative variable current $U = U_0\text{Sech}\left[\varepsilon^2(x - 200)\right]$, $U_0 = -0.1$, is presented in Fig. 1b. The modulation instability develops far more quickly on opposing current and reaches deeper stages of modulation. The energetic process is described as follows. The basic Stokes wave (I) absorbs energy from the counter current U and its steepness increases. This in turn accelerates the wave instability; there is a corresponding increase in energy flow to the most unstable sideband modes (II) and (III). Wave refraction by current is acting simultaneously with nonlinear wave interactions. The linear modulation model (Gargett and Hughes, 1972; Lewis et al., 1974) assumes the independent variations of harmonics with current and gives much larger maximum amplitude of the carrier wave (IV). It just adsorbs energy from the adverse current.

The region of the most developed instability corresponds to the spatial location of the maximum of the negative current (Fig. 1c). As one can see from Fig. 1b, c, the initial stage of wave-current interaction is characterized by the dominant process absorbing of energy by waves where all three waves grow simultaneously. Initial growth of side band modes (Fig. 1c) leads to a deeper modulated regime. Increasing of wave steepness in turn accelerates instability and finally these two dominate processes alternate. Correspond-
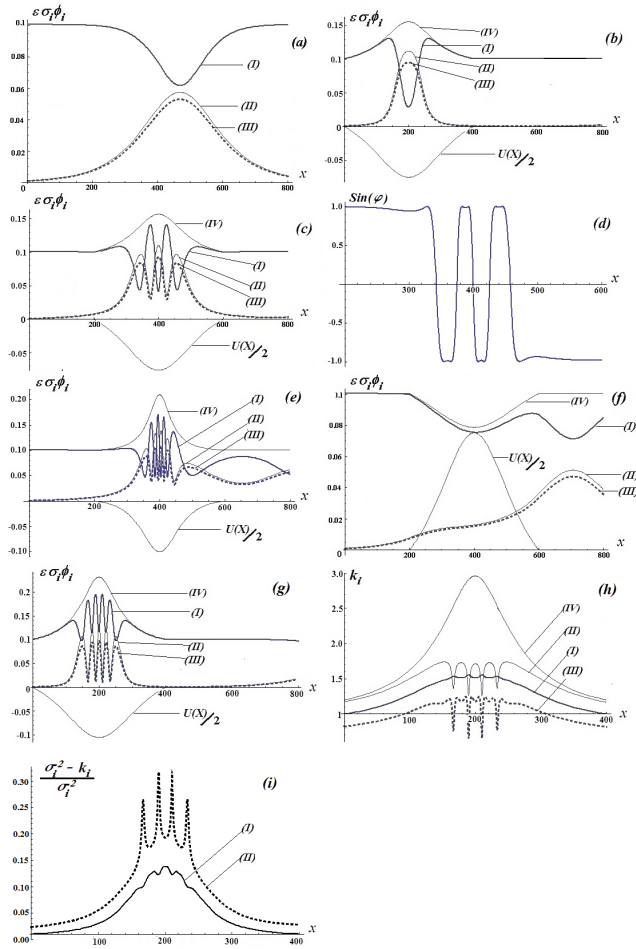
Figure 1. (a) BF instability without current. **(b)** and **(c)** modulation of surface waves by adverse current $U = U_0 \text{Sech}\left[\varepsilon^2(x - x_0)\right]$, ($U_0 = -0.15$); **(b)** $x_0 = 200$ and **(c)** $x_0 = 400$. **(d)** phase difference function $\varphi[X] = 2\theta_1[X] - \theta_0[X] - \theta_2[X]$, $\theta_1[0] = 0$; $\theta_0[0] = \theta_2[0] = -\pi/4$; **(e)** modulation of surface waves by adverse current $U = U_0 Sech\left[2\varepsilon^2(x - x_0)\right]$, ($U_0 = -0.2$), **(f)** modulation instability for following current ($U_0 = 0.16, x_0 = 400$). **(g)** and **(h)** functions of wave amplitude and wave number, respectively, for $U_0 = -0.2$. (I), (II), (III) amplitude envelopes of the carrier, superharmonic and subharmonic waves, respectively. (IV) linear solution for the carrier envelope. The initial steepness of the carrier wave is $\varepsilon = 0.1$, side band initial amplitudes are equal to 0.1ε. **(i)** Relative distortion of the linear dispersion relation for the case **(g)**, (I) – carrier, (II) – higher side band.

effects and nonlinearity. Maybe the almost resonance conditions are totally destroyed in this case due to large detuning (Shrira and Slunyaev, 2014)?

To clarify this property we present the behavior of phase-shift difference function $\varphi[X] = 2\theta_1 - \theta_0 - \theta_2$ (Fig. 1d) corresponding to waves modulation shown in Fig. 1c. Intensity of nonlinear energy transfer is mostly defined by this function together with wave amplitudes (see Eqs. 17, 20). The results look rather surprising – several strong phase jumps take place with corresponding changes of the wave energy flux direction. Nevertheless, we see an intensive energy exchange in the entire interaction zone. Quasi-resonant conditions are satisfied locally in space with a relatively small detuning factor. Qualitatively similar behavior of phase-shift function we found also for other regimes of wave modulation.

The typical scenario of wave interaction with co-propagating current is presented in Fig. 1f. The modulation instability is depressed by the following current $U(X) > 0$ and the resonant sideband modes develop at almost two time's longer distance in comparison with the evolution without current.

Regimes of modulation presented in Fig. 1a–c demonstrate the strictly symmetrical behavior with respect to the current peak and wave train returns to its initial structure after interaction with current. The modulation equations permit symmetrical solutions for the symmetrical current function, but, outside of interaction zone the nonlinear periodic waves are defined by the boundary conditions and the constant Stokes wave is only one of such possibilities. The symmetrical behavior is typical for a sufficiently slow-varying current. We present in Fig. 1e the example of asymmetrical wave modulation for the same wave initial characteristics as for Fig. 1c and 2 times shorter space scale of the current. At the exit of wave-current interaction zone we mention three waves system with comparable amplitudes and periodic energy transfer.

The increasing strength of the opposing flow ($U_0 = -0.2$) results in deeper modulation of waves and more frequent mutual oscillations of the amplitudes (Fig. 1g). There are essential oscillations of wave-number functions of the sideband modes (II) and (III) (Fig. 1h) owing to the nonlinear dispersion properties of waves. We mention also that the wave number of the carrier wave in the linear model (IV) is much higher than that in the nonlinear model (I). The width of the wave-number spectrum of the wave train in the nonlinear model locally increases to almost twice that of the initial width. To give an idea about the strength of nonlinearity, we present in Fig. 1i the relative distortion of the linear dispersion relation for different modes. As one can see the effect of nonlinearity for the carrier (at maximum is about 10 %) is much less compared to side bands (at peak is more than 30 %). The main impact of nonlinearity comes from the amplitude Stokes dispersion.

To estimate the possibility of generating large transient waves, we employ the model and calculate the maximum
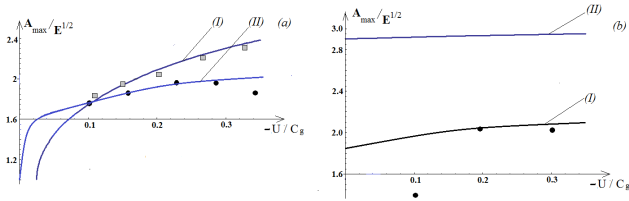
ingly, the triggering of this complicated process essentially depends on the displacement of the current maximum.

Quasi-resonance interaction of waves in the presence of variable current causes some crucial questions about its detuning properties. Absolute frequencies for the stationary modulation satisfy the resonance conditions (Eq. 7) for the entire region of interaction. But the local wave numbers and intrinsic frequencies are substantially variable due to current

Figure 2. Nondimensional maximum wave amplitude as a function of $-U/C_g$, where C_g is the group velocity of the carrier wave and $E^{1/2}$ is the local standard deviation of the wave envelope. **(a)** experiments conducted by Toffoli et al. (2013) for carrier wave of period $T = 0.8\,s$ (wavelength $\lambda \cong 1\,m$), initial steepness $k_1 a_1 = 0.063$, and frequency difference $\Delta\omega/\omega_1 = 1/11$, initial amplitudes of side bands equal to 0.25 times the amplitude of the carrier wave. Solid dots show measurements made using a flume at Tokyo University and squares show results obtained at Plymouth University. Line (I) shows the prediction made using Eq. (2) (Toffoli et al., 2013) while line (II) shows the model prediction. **(b)** case T11 in Ma et al. (2013) for carrier-wave frequency $\omega_1 = 1\,Hz$, initial steepness $k_1 a_1 = 0.115$, initial amplitudes of side bands equal to 0.05 times the amplitude of the carrier wave and frequency difference $\Delta\omega/\omega_1 = 0.44 a_1 k_1$. Solid dots show measurements. Line (I) shows the model prediction, while line (II) shows the prediction made using Eq. (2) (Toffoli et al., 2013).

amplification of the amplitudes of surface waves generated in still water and then undergo a current quickly raised to a constant value $-U$. The boundary conditions for the unperturbed waves were taken from experiments conducted by Toffoli et al. (2013) and Ma et al. (2013). Results of the calculations are presented in Fig. 2a and b.

Our simulations confirm that initially stable waves in experiments of Toffoli et al. (2013) undergo a modulationally unstable process and wave amplification in the presence of adverse current. Maximum amplification reasonably corresponds to results of experiments at the Tokyo University Tank for moderate strength of current. Maximum of nonlinear focusing in dependence on the value of current is weaker compare to the model of Toffoli et al. (2013).

Experiments of Ma et al. (2013) (Fig. 2b) show that the development of the modulational instability for a gentle wave and relatively weak adverse current ($U/C_g \sim -0.1$) (see the first experimental point) is limited due to the presence of dissipation. Our model simulations are in good agreement with the experimental values for the moderate values of adverse current $-U/C_g \sim 0.2 - 0.4$. Results of Toffoli et al. (2013) notably overestimate the maximum of wave amplification.

4 Wave propagation under the blocking conditions of strong adverse current

Stokes waves with sufficiently high initial steepness ε under the impact of strong blocking adverse current ($U(X) < -C_g$) will inevitably reach the breaking threshold for the steepness

of water waves. We employ the adjusted weakly nonlinear dissipative model of Tulin (1996), Tulin and Li (1999) and Hwung et al. (2011) to describe the effect of breaking on the dynamics of the water wave.

Dual non-conservative evolution equations for wave energy density $E = 1/2 g\eta^2$ and wave momentum $M = E/c = E/(\omega/k)$, or, correspondingly, for energy E and celerity c were rigorously derived (Tulin and Li, 1999) using the variational approach: a modified Hamiltonian principle involving the modulating wave Lagrangian plus a work function representing the nonconservative effects of wave breaking. It was also shown that these dual equations correspond to the complex NLS equation, as modified by the non-conservative effects, i.e. to energy and dispersion equations. Wave breaking effects were characterized by the energy dissipation rate D_b and momentum loss rate M_b.

An analysis of fetch laws parameterized by Tulin (1996) reveals that the rate of energy loss D_b due to breaking is of fourth order of the wave amplitude:

$$D_b/E = \omega D \eta^2 k^2,$$

and $D = O(10^{-1})$ is a small empirical constant. Momentum-loss rate M_b was quantified in terms of energy dissipation rate D_b and parameterized in such a way that

$$c M_b = (1 + \gamma) D_b,$$

where γ is empirical coefficient, which is varied in the range $\gamma = 0.4 - 0.7$. Strong plunging breaking corresponds to $\gamma = 0.4$ and weak to $\gamma = 0.7$. In all our numerical simulations was chosen $\gamma = 0.4$, $D = 0.1$.

Tulin and Waseda (1999), through consideration of a multimodal wave system evolving from a carrier wave and two side bands, showed that energy downshifting during breaking is determined by the balance between momentum and dissipation losses, suitably parameterized by the parameter γ:

$$\frac{\partial}{\partial t}(E_0 - E_2) = \gamma D_b/(\delta\omega/\omega),$$

where E_0, E_2 – energy densities of the sub and super harmonics, respectively. The parametric value γ was found to be positive $\gamma > 0$ and providing the long term downshifting.

The sink of energy D_b and momentum M_b due to wave breaking leads to additional terms at the right sides of the wave energy Eq. (20) and dispersive Eq. (16) for each of the waves. Tulin (1996) suggested using sink terms along the entire path of wave interaction with the wind. The wave dissipation function for the adjusted model (Hwung et al., 2011) includes also the wave steepness threshold function

$$H\left[\frac{\left|\varepsilon \sum \sigma_i \phi_i k_i\right|}{A_S} - 1\right],$$

where H is the Heaviside unit step function and A_S is the threshold value of the combined wave steepness $\varepsilon \sum \sigma_i \phi_i k_i$,

is applied to calculate energy and momentum losses in high steepness zones. In our computations the threshold $A_S = 0.32$ was chosen.

The dispersion relations (16) and wave energy laws (20) including break dissipation take the form

$$
\begin{cases}
\sigma_0^2 = k_0 + \varepsilon^2 \sigma_0^3 (\varphi_0^2 \sigma_0^5 + \varphi_1^2 \sigma_1^3 (2\sigma_1^2 - \sigma_0 \sigma_1 + \sigma_0^2) \\
\quad + \varphi_2^2 \sigma_2^3 (2\sigma_2^2 - \sigma_0 \sigma_2 + \sigma_0^2)) + \\
\frac{\varepsilon^2 \varphi_1^2 \varphi_2 \sigma_0^3 \sigma_2^2}{\varphi_0} (2\sigma_1^3 - 2\sigma_1^2 \sigma_2 + 2\sigma_1 \sigma_2^2 - \sigma_2^3) Cos[\phi] + \varepsilon^2 \\
H[\chi] D \begin{Bmatrix} Sin[\phi] \varphi_1^2 \varphi_2 / \varphi_0 k_0^4 + 8\gamma \varepsilon^2 X (\varphi_0^2 + \varphi_1^2 + \varphi_2^2) - \\ 4\gamma \varphi_1^2 \varphi_2 / \varphi_0 Sin[\phi] \end{Bmatrix}, \\[4mm]
\sigma_2^2 = k_2 + \varepsilon^2 \sigma_2^3 (\varphi_2^2 \sigma_2^5 + \varphi_0^2 \sigma_0^3 (2\sigma_0^2 - \sigma_0 \sigma_2 + \sigma_2^2) \\
\quad + \varphi_1^2 \sigma_1^3 (2\sigma_1^2 - \sigma_1 \sigma_2 + \sigma_2^2)) + \\
\frac{\varepsilon^2 \varphi_1^2 \varphi_0 \sigma_2^3 \sigma_0^2}{\varphi_2} (2\sigma_1^3 - 2\sigma_0 \sigma_1^2 + 2\sigma_0^2 \sigma_1 - \sigma_0^3) Cos[\phi] + \varepsilon^2 \\
H[\chi] D \begin{Bmatrix} Sin[\phi] \varphi_1^2 \varphi_0 / \varphi_2 k_2^4 + 8\gamma \varepsilon^2 X (\varphi_0^2 + \varphi_1^2 + \varphi_2^2) + \\ 4\gamma \varphi_1^2 \varphi_0 / \varphi_2 Sin[\phi] \end{Bmatrix}, \\[4mm]
\sigma_1^2 = k_1 + \varepsilon^2 \sigma_1^3 (\varphi_1^2 \sigma_1^5 + \varphi_0^2 \sigma_0^3 (2\sigma_0^2 - \sigma_0 \sigma_1 + \sigma_1^2) \\
\quad + \varphi_2^2 \sigma_2^3 (\sigma_1^2 - \sigma_1 \sigma_2 + 2\sigma_2^2)) + \\
\varepsilon^2 \varphi_0 \varphi_2 \sigma_0 \sigma_1^2 \sigma_2 (\sigma_0^4 - \sigma_0^3 \sigma_1 - \sigma_0 \sigma_1 (\sigma_1 - \sigma_2)^2 \\
\quad + \sigma_0^2 (\sigma_1^2 - \sigma_1 \sigma_2 + 2\sigma_2^2) + \\
\sigma_2 (-\sigma_1^3 + \sigma_1^2 \sigma_2 - \sigma_1 \sigma_2^2 + \sigma_2^3)) Cos[\phi] + \varepsilon^2 \\
H[\chi] D \begin{Bmatrix} -2Sin[\phi] \varphi_2 \varphi_0 k_1^4 + 8\gamma \varepsilon^2 X (\varphi_0^2 + \varphi_1^2 + \varphi_2^2) + \\ 4\gamma \varphi_2 \varphi_0 Sin[\phi] \end{Bmatrix},
\end{cases}
$$

(21)

where $\chi = \left| \varepsilon \sum \sigma_i \phi_i k_i \right| / A_S - 1$, and

$$
\begin{cases}
[(U(X) + \frac{1}{2\sigma_0}) \varphi_0^2 \sigma_0]_X = \varepsilon \varphi_1^2 \varphi_2 \varphi_0 \sigma_1^3 \sigma_2^2 (2\sigma_1^3 - 2\sigma_1^2 \sigma_2 \\
\quad + 2\sigma_1 \sigma_2^2 - \sigma_2^3) Sin[\phi] \varepsilon + H[\chi] D \\
\begin{Bmatrix} -k_0^4 \varphi_1^2 \varphi_2 \varphi_0 Cos[\phi] - k_0^4 \varphi_0^2 (\varphi_0^2 + 2\varphi_1^2 + 2\varphi_2^2) + \\ 4\gamma \varphi_0^2 k_0^4 (\varphi_1^2 + \varphi_2^2 + \varphi_1^2 \varphi_2 / \varphi_0 Cos[\phi]) \end{Bmatrix}, \\[4mm]
[(U(X) + \frac{1}{2\sigma_2}) \varphi_2^2 \sigma_2]_X = \varepsilon \varphi_1^2 \varphi_2 \varphi_0 \sigma_1^3 \sigma_0^2 (2\sigma_1^3 - 2\sigma_0 \sigma_1^2 \\
\quad + 2\sigma_0^2 \sigma_1 - \sigma_0^3) Sin[\phi] + \varepsilon H[\chi] D \\
\begin{Bmatrix} -k_2^4 \varphi_1^2 \varphi_2 \varphi_0 Cos[\phi] - k_2^4 \varphi_2^2 (\varphi_2^2 + 2\varphi_0^2 + 2\varphi_1^2) + \\ 4\gamma \varphi_2^2 k_2^4 (\varphi_1^2 + \varphi_0^2 + \varphi_1^2 \varphi_0 / \varphi_2 Cos[\phi]) \end{Bmatrix}, \\[4mm]
[(U(X) + \frac{1}{2\sigma_1}) \varphi_1^2 \sigma_1]_X = -\varepsilon \varphi_1^2 \varphi_2 \varphi_0 \sigma_0 \sigma_1^2 \sigma_2 (\sigma_0^4 - \sigma_0^3 \sigma_1 \\
\quad - \sigma_0 \sigma_1 (\sigma_1 - \sigma_2)^2 + \sigma_0^2 (\sigma_1^2 - \sigma_1 \sigma_2 + 2\sigma_2^2) - \sigma_2 (\sigma_1^3 \\
\quad - \sigma_1^2 \sigma_2 + \sigma_1 \sigma_2^2 - \sigma_2^3)) Sin[\phi] + \varepsilon H[\chi] D \\
\begin{Bmatrix} -2k_1^4 \varphi_1^2 \varphi_2 \varphi_0 Cos[\phi] - k_1^4 \varphi_1^2 (\varphi_1^2 + 2\varphi_0^2 + 2\varphi_2^2) + \\ 4\gamma \varphi_1^2 k_1^4 ((\varphi_2^2 - \varphi_0^2) + \varphi_2 \varphi_0 Cos[\phi]) \end{Bmatrix}.
\end{cases}
$$

(22)

Wave breaking leads to permanent (not temporal) frequency downshifting at a rate controlled by breaking process. A crucial aspect here is the cooperation of dissipation and near-neighbor energy transfer in the discretized spectrum acting together.

The numerical simulations for initially high steepness waves ($\varepsilon = 0.25$) propagation with wave breaking dissipation is presented in Fig. 3a–c. We calculate the amplitudes of surface waves on linearly increasing opposing current $U(x) = -U_0 x$ with different strength U_0. The most unstable regime was tested for frequency space $\Delta\omega_\pm / \omega_1 \sim \varepsilon$, initial side bands amplitudes equal to 0.05 times the amplitude of the carrier wave and most effective initial phases $\theta_1(0) = 0, \theta_0(0) = \theta_2(0) = -\pi/4$.

A very weak opposite current $U_0 = 2.5\,10^{-4}$ (Fig. 3a) has a pure impact on wave behavior: it finally results in almost bichromatic wave train with two dominant waves: carrier and lower side band. Frequency downshift here is not clearly seen. Two times stronger current case with $U_0 = 5 \times 10^{-4}$ is presented in Fig. 3b. We note some tendency to final energy downshift to the lower side band. Really strong permanent downshift with total domination of the lower side band is seen for two times more strong current $U_0 = 10^{-3}$ (Fig. 3c).

We also performed numerical simulations for the boundary conditions and the form of the variable current obtained in two series of experiments conducted by Chavla and Kirby (2002) and Ma et al. (2010).

Data for the wave blocking regime in experiments conducted by Chavla and Kirby (2002) are taken from their Test 6 (Fig. 11). The experimental results of test 6 and our numerical simulation results are compared in Fig. 4. A surface wave with initially high steepness ($A_1 k_1 = 0.296$) and period $T = 1.2\,\text{s}$ meets adverse current with increasing amplitude.

The model simulations results have distinctive features that agree reasonably well with the results of experiments:

– initial symmetrical growth of the main sidebands with frequencies $f_0 = 0.688\,\text{Hz}$, $f_2 = 0.978\,\text{Hz}$ at distances up to $k_1 x < -2$;

– asymmetrical growth of sidebands beginning at ($k_1 x \approx -2$) and downshifting of energy to the lower sideband;

– energy transfer at very short spatial distances and several increases in the lower sideband amplitude just on a half meter length $k_1 x \in (-2, 0)$;

– a depressed higher frequency band and primary wave;

– an almost permanent increase in the lowest subharmonic along the tank;

– sharp accumulation of energy by the lowest subharmonic wave during interaction with increasing opposing current;

– final permanent downshifting of the wave energy.

Modulation evolution of breaking waves in experiments of Ma et al. (2010) for the most intriguing case 3 are presented in Fig. 5 together with the results of our numerical computations. A primary wave with period $T = 1 s$ and steepness $A_1 k_1 = 0.18$ meets linearly increasing opposing current that
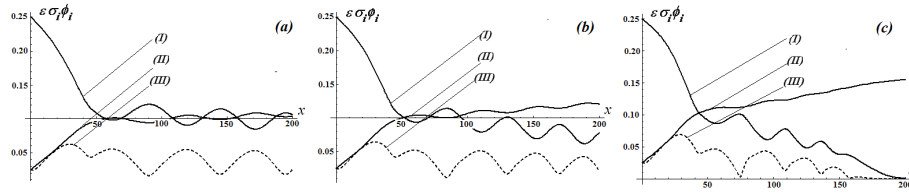
Figure 3. Modulation of surface waves by the adverse current $U = U_0 x$. **(a)** $U_0 = -2.5\,10^{-4}$, **(b)** $U_0 = -5\,10^{-4}$, **(c)** $U_0 = -10^{-3}$. (I), (II), (III) – amplitude envelopes of the carrier, subharmonic and superharmonic waves, respectively. Initial wave steepness $\varepsilon = 0.25$, side bands amplitudes equal to 0.05 times the amplitude of the carrier.
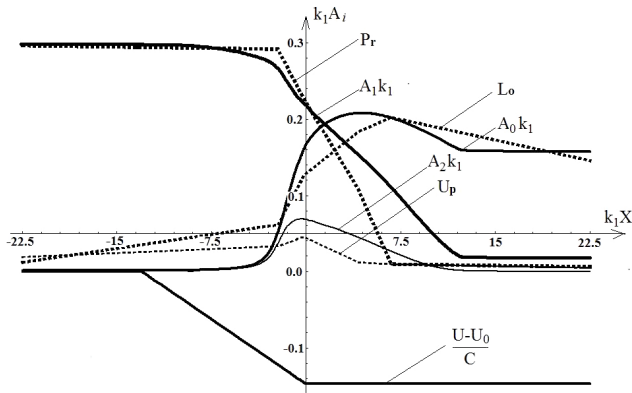

Figure 4. Dashed curves show the amplitudes of the waves for primary (Pr), lower (Lo) and upper (Up) sidebands obtained experimentally by Chavla and Kirby (2002). The solid lines (A_1, A_0, A_2) are wave amplitudes calculated in modeling. $(U - U_0)/C$ is the no-dimensional variable current, where C is the initial phase speed of the carrier wave, $U_0 = -0.32\,m/s$; $k_1 = 4.71/m$, $C = 1.44\,m/s$, $T = 1.2\,s$.
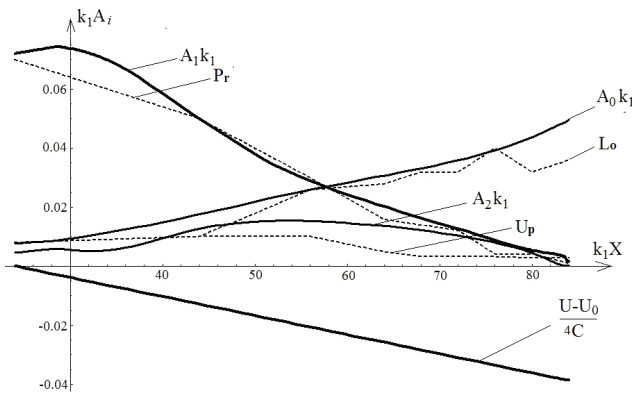

Figure 5. Dashed curves show amplitudes of the waves for primary (Pr), lower (Lo) and upper (Up) sidebands obtained from experiments conducted by Ma et al. (2010). The solid lines (A_1, A_0, A_2) are the wave amplitudes calculated in modeling. $(U - U_0)/(4C)$ shows the no-dimensional variable current, where C is the initial phase speed of the primary wave, $U_0 = -0.25\,m/s$; $k_1 = 4.1/m$, $C = 1.56\,m/s$, $T = 1\,s$.

finally exceeds the threshold to be a linear blocking barrier for the primary wave $U(x) < -1/4C$. In experiments, sideband frequencies arose ubiquitously from the background noise of the flume. In numerical simulations, the sidebands were slightly seeded at frequencies corresponding to the most unstable modes. The wave-breaking region in this experimental case ranged from $k_1 x = 52$ to $k_1 x = 72$. The lower sideband amplitude grew with increasing distance at the expense of the primary wave, while there was little change in the higher sideband energy. There was an effective frequency downshift following initial breaking ($k_1 x = 56$). The modeling results agree reasonably well with the experimental data.

5 Conclusions

The evolution of a Stokes wave and its two main sidebands on a slowly varying unidirectional steady current gives rise to modulation instability with special properties. Interaction with countercurrent accelerates the growth of sideband modes on much shorter spatial scales. In contrast, wave instability on the following current is sharply depressed. Amplitudes and wave numbers of all waves vary enormously in the presence of strong adverse current. The increasing strength of the opposing flow results in deeper modulation of waves and more frequent mutual oscillations of the waves amplitudes.

Large transient or freak waves with amplitude and steepness several times larger than those of normal waves may form during temporal nonlinear focusing of waves accompanied by energy income from sufficiently strong opposing current. The amplitude of a rough wave strongly depends on the ratio of the current velocity to group velocity.

Interaction of initially steep waves with the strong blocking adverse current results in intensive energy exchange between components and energy downshifting to the lower sideband mode accompanied by active breaking. A more stable long wave with lower frequency can overpass the blocking barrier and accumulate almost all the wave energy of the packet. The frequency downshift of the energy peak is permanent and the system does not revert to its initial state.

The model simulations satisfactorily agree with available experimental data on the instability of waves on blocking adverse current and the generation of rough waves.

References

Benjamin, T. B. and Feir, J. E.: Instability of periodic wavetrains in
nonlinear dispersive systems, J. Fluid Mech., 27, 417–430, 1967.

Bridges, T. and Dias, F.: Enhancement of the Benjamin-Feir insta-
bility with dissipation, Phys. Fluids, 19, 104–104, 2007.

Chavla, A. and Kirby, J.: Experimental study of breaking waves on a
blocking current, Proc. 26th International Conference on Coastal
Engineering, Copenhagen, 22–26 June, 759–772, 1998.

Chavla, A. and Kirby, J.: Monochromatic and random wave break-
ing at block points, J. Geophys. Res., 107, 4.1–4.19, 2002.

Chabchoub, A., Akhmediev, N., and Hoffmann, N.: Experimental
study of spatiotemporally localized surface gravity water waves,
Phys. Rev. E., 86, 016311, doi:10.1103/PhysRevE.86.016311,
2012.

Chiang, W. and Hwung, H.: Large transient waves generated
through modulational instability in deep water, J. Hydrodynam.,
22, 114–119, 2010.

Dias, F. and Kharif, C.: Nonlinear gravity and capillary-gravity
waves, Annu. Rev. Fluid Mech., 31, 301–346, 1999.

Donato, A. N., Peregrine, D. H., and Stocker, J. R.: The focusing
of surface. waves by internal Waves, J. Fluid Mech., 384, 27–58,
1999.

Duin, C.: The effect of non-uniformity of modulated wavepackets
on the mechanism of Benjamin–Feir instability, J. Fluid Mech.,
399, 237–249, 1999.

Dysthe, K. B.: Note on a modification to the nonlinear Schrodinger
equation for application to deep water waves, Proc. R. Soc. A,
369, 105–114, 1979.

Gargett, A. E. and Hughes, B. A.: On the interaction of surface and
internal waves, J. Fluid Mech., 52, 179–191, 1972.

Gerber, M.: The Benjamin–Feir instability of a deep water Stokes
wave packet in the presence of a non-uniform medium, J. Fluid
Mech., 176, 311–332, 1987.

Hara, T. and Mei, C.: Frequency downshift in narrowbanded surface
waves under the influence of wind, J. Fluid Mech., 130, 429–477,
1991.

Hjelmervik, K. B. and Trulsen, K.: Freak wave statistics on collinear
currents, J. Fluid Mech., 637, 267–284, 2009.

Hwung, H., Chiang W., and Hsiao S.: Observations on the evolution
of wave modulation, Proc. R. Soc. London, Ser. A, 463, 85–112,
2007.

Hwung, H., Yang, R., and Shugan, I.: Exposure of internal waves
on the sea surface, J. Fluid Mech., 626, 1–20, 2009.

Hwung, H., Chiang W., Yang, R., and Shugan, I.: Threshold Model
on the Evolution of Stokes Wave Side-Band Instability, Eur. J.
Mech. B/Fluids, 30, 147–155, 2011.

Janssen, P.: Nonlinear four-wave interactions and freak waves, J.
Phys. Oceanogr., 33, 863–884, 2003.

Janssen, T. and Herbers, T.: Nonlinear Wave Statistics in a Focal
Zone, J. Phys. Oceanogr., 39, 1948–1964, 2009.

Kharif, C. and Pelinovsky, E.: Freak waves phenomenon: physical
mechanisms and modelling, in: Waves in Geophysical Fluids:
CISM Courses and Lectures 489, edited by: Grue, J. and Trulsen,
K., 107–172, Springer, 2006.

Lake, B. M. and Yuen, H. C.: A new model for nonlinear wind
waves. Part 1. Physical model and experimental evidence, J.
Fluid Mech., 88, 33–62, 1978.

Landrini, M., Oshri, O., Waseda, T., and Tulin, M. P.: Long time
evolution of gravity wave systems, in: Proc. 13th Intl Workshop
on Water Waves and Floating Bodies, edited by: Hermans, A. J.,
Alphen aan den Rijn, 75–78, 1998.

Lavrenov, I. V.: The wave energy concentration at the Agulhas cur-
rent off South Africa, Nat. Hazards, 17, 117–127, 1998.

Lewis, J. E., Lake, B. M., and Ko, D. R.: On the interaction of in-
ternal waves and surface gravity waves, J. Fluid Mech., 63, 773–
800, 1974.

Lo, E. and Mei, C. C.: A numerical study of water-wave modulation
base on a higher-order nonlinear Schrodinger equation, J. Fluid
Mech., 150, 395–416, 1985.

Longuet-Higgins, M., and Stewart, R.: Radiation stresses in water
waves: a physical discussion, with applications, Deep-Sea Res.,
11, 529–562, 1964.

Ma, Y., Dong, G., Perlin, M., Ma, X., Wang, G., and Xu, J.: Labo-
ratory observations of wave evolution, modulation and blocking
due to spatially varying opposing currents, J. Fluid Mech., 661,
108–129, 2010.

Ma, Y., Ma, X., Perlin, M., and Dong, G.: Extreme waves generated
by modulational instability on adverse currents, Phys. Fluids, 25,
114109, doi:10.1063/1.4832715, 2013.

Mei, C., You, D., and Stiassnie, M.: Theory and Applications of
Ocean Surface Waves, World Scientific, Hackensack (N.J.) ,
2009.

Moreira, R. and Peregrine, D.: Nonlinear interactions between
deep-water waves and currents, J. Fluid Mech., 691, 1–25, 2012.

Onorato, M., Proment, D., and Toffoli, A.: Triggering rogue
waves in opposing currents, Phys. Rev. Lett., 107, 184502,
doi:10.1103/PhysRevLett.107.184502, 2011.

Osborne, A.: The random and deterministic dynamics of "rogue
waves" in unidirectional, deep-water wave trains, Mar. Struct.,
14, 275–293, 2001.

Osborne, A. R., Onorato M., and Serio M.: The nonlinear dynam-
ics of rogue waves and holes in deep-water gravity wave trains,
Phys. Lett. A, 275, 386–393, 2000.

Peregrine, D. H.: Interaction of water waves and currents, Adv.
Appl. Mech., 16, 9–117, 1976.

Phillips, O. M.: The Dynamics of the Upper Ocean, Cambridge Uni-
versity Press, 1977.

Ruban, V.: On the Nonlinear Schrödinger Equation for Waves on a
Nonuniform Current, JETP Letters, 95, No. 9, 486–491, 2012

Segur, H., Henderson, D., Hammack, J., Li, C.-M., Phei, D., and
Socha, K.: Stabilizing the Benjamin–Feir instability, J. Fluid
Mech., 539, 229–271, 2005.

Shemer, L.: On Benjamin-Feir instability and evolution of a non-
linear wave with finite-amplitude sidebands, Nat. Hazards Earth

Syst. Sci., 10, 2421–2427, doi:10.5194/nhess-10-2421-2010, 2010.

Shemer, L., Kit, E., and Jiao, H.: An experimental and numerical study of the spatial evolution of unidirectional nonlinear water-wave groups, Phys. Fluids, 14, 3380–3390, 2002.

Shrira, V. and Slunyaev, A.: Trapped waves on jet currents: asymptotic modal approach, J. Fluid Mech., 738, 65–104, 2014.

Shugan, I. and Voliak, K.: On phase kinks, negative frequencies and other third order peculiarities of modulated surface waves, J. Fluid Mech., 368, 321–338, 1998.

Slunyaev, A. and Shrira, V.: On the highest non-breaking wave in a group: fully nonlinear water wave breathers versus weakly non-linear theory, J. Fluid Mech., 735, 203–248, 2013.

Smith, R.: Reflection of short gravity waves on a non-uniform current, Math. Proc. Cambridge Philos. Soc., 78, 517–525, 1975.

Stiassnie, M. and Shemer, L.: On the interaction of four water-waves, Wave Motion, 41, 307–328, 2005.

Stocker, J. R. and Peregrine, D. H.: Three-dimensional surface. waves propagating over long internal waves, European J. Mech. B/Fluids, 18, 545–559, 1999.

Tanaka, M.: Maximum amplitude of modulated wavetrain, Wave Motion, 12, 559–568, 1990.

Toffoli, A., Waseda, T., Houtani, H., Kinoshita, T., Collins, K., Proment, D., and Onorato, M.: Excitation of rogue waves in a variable medium: An experimental study on the interaction of water waves and currents, Phys. Rev. E, 87, 051201, doi:10.1103/PhysRevE.87.051201, 2013.

Trulsen, K. and Dysthe, K.: Frequency down-shift through self modulation and breaking, in: Water Wave Kinematics, edited by: Torum, A. and Gudmestad, T., 561–572, Kluwer, 1990.

Trulsen, K., Kliakhandler, I., Dysthe, K., and Velarde, M.: On weakly nonlinear modulation of waves on deep water, Phys. Fluids, 12, 2432–2437, 2000.

Tulin, M. P.: Breaking of ocean waves and downshifting, in: Waves and Nonlinear Processes in Hydrodynamics, edited by: Grue, J., Gjevik, B., and Weber, J. E., 177–190, Kluwer, 1996.

Tulin, M. P. and Li, J. J.: The nonlinear evolution of wind driven, breaking ocean waves: mathematical description, OEI. Tech. Rpt., No. 99–202, 1999.

Tulin, M. P. and Waseda, T.: Laboratory observations of wave group evolution, including breaking effects, J. Fluid Mech., 378, 197–232, 1999.

White, B. and Fornberg,B.: On the chance of freak waves at sea, J. Fluid Mech., 355, 113–138, 1998.

Whitham, G. B.: Linear and Nonlinear Waves, John Wiley & Sons, 1974.

Yuen, H. C. and Lake, B. M.: Nonlinear dynamics of deep-water gravity waves, in: Advances in Applied Mechanics, 22, 67–229, Academic Press, 1982.

Zakharov, V., Dyachenko, A., and Prokofiev, A.: Freak waves as nonlinear stage of Stokes wave modulation instability, European J. Mech. B/Fluids, 25, 677-692, 2006.